A NEW MEASUREMENT OF THE COSMIC RAY ENERGY SPECTRUM BETWEEN 3×10^{15} eV AND 3×10^{16} eV

A.G. Gregory, J.R. Patterson and R.J. Protheroe
Department of Physics, University of Adelaide
Adelaide, South Australia, 5001.

ABSTRACT

We give the results of a new Cerenkov photon density spectrum measurement and present our derivation of the primary cosmic ray energy spectrum for energies from 3×10^{15}eV to 3×10^{16}eV.

1. Introduction. In a previous paper, Protheroe and Patterson[1] examined the information available from various types of Cerenkov light photon density spectrum measurements and proposed a conceptually simple but powerful experiment. From simulations, it was found that the photon density spectrum of nearly vertical air showers observed by a system of two detectors separated by 350 m was independent of nuclear mass composition and depended only on the primary energy spectrum. On the other hand, a system of two detectors close together (or a single detector) would be sensitive to the composition. By making these two measurements then, it is possible to determine the energy spectrum and obtain information about composition.

In practice, the experiment is complicated by the necessity to observe only near-vertical showers and to know the acceptance solid angle of the system. Either one severely collimates the detectors (or uses mirrors) or one allows the detectors an unrestricted field of view and selects the shower arrival directions by another technique, e.g. the use of a third detector and timing coincidence. Since the simulations in ref. 1 were made for unshielded detectors we have used the latter approach in order to avoid cutting out Cerenkov light produced in the later stages of development.

2. Techniques. Our system consisted of three 175 mm diameter 9623B photomultipliers (PMT), each with a collimator to cut out background light beyond 45° from the PMT axis. Full details of the experiment will be published elsewhere. In the energy spectrum measurement, two of these detectors were used to record photon densities and were separated by 350 m. The third detector was offset by 100 m to enable a coincidence timing system with pre-determined pulse widths and delays from each detector to restrict air shower arrival directions to a well defined solid angle (0.32 sr) centred about the zenith. For the composition measurement the density detectors were moved to 100 m separation, and the third detector to 31 m. The pulse widths and delays were adjusted to give an acceptance solid angle of 0.29 sr.

Calibrations were made throughout the night with a temperature stabilised green LED pulser mounted near the rim of the mechanical collimator to compensate for gain drifts. An absolute calibration of a blue LED system was made in the laboratory by comparing the PMT output with that due to a known flux of Cerenkov light photons produced by single muons passing through BK7 glass and has been described by Gregory et al[2]. This was used to calibrate the green pulsers in situ.

3. Observations. Initially, the fast PMT outputs were shaped by Ortec 485 main amplifiers, and the pulse heights were sampled and digitized. The system was tested at the Buckland Park field station and moved to a better observing site at Alice Springs for observations in May/June 1984. Alice Springs is at an elevation of 540 m and, for comparison with the simulations which were made for sea level, the detectors were tilted at 20° to the vertical in order to see showers at the same stages of development as in sea level observations. The pulse from the offset detector was appropriately delayed to tilt the acceptance solid angle for air showers by the same amount.

The results of this run for the May/June 1984 new moon period are shown in Fig. 1 by the open circles (details of the analysis are given below). With the rather slow electronics we were using, and the large field of view of the mechanical collimators, the results were subject to a fluctuating night sky noise component which became important below $\sim 3\times10^5$ photons m^{-2}. Estimates of the effect on the expected power law photon density spectra enabled approximate corrections to be made to these data and are indicated by the solid circles.

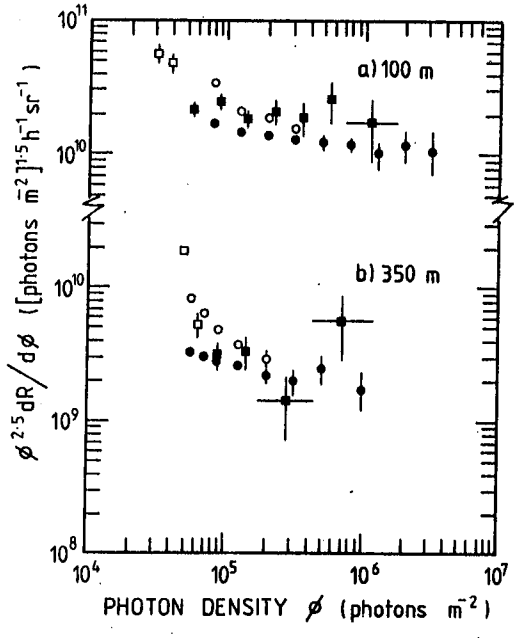

Fig. 1. Differential photon density spectra observed with (a) the 100 m system and (b) the 350 m system. Observations made at Alice Springs are indicated by open circles and are subject to biasses due to night sky noise below $\sim 3\times10^5$ photons m^{-2}. An approximate correction based on the characteristics of the system and an assummed night sky brightness of 6.4×10^{11} photons m^{-2} s^{-1} sr^{-1} has been made and these corrected data replotted as filled circles. Observations made subsequently at Woomera are indicated by filled squares and are subject to biasses due to night sky noise below $\sim 5\times10^4$ photons m^{-2} (open squares).

Following the analysis of these observations, the electronics were redesigned around a LeCroy 2249SG Integrating ADC and the mechanical collimators were extended to reduce the sky background. The acceptance solid angle of the system for air showers was also reduced (to 0.082 sr and 0.11 sr for the 350 m and 100 m systems respectively) so that the mechanical collimators did not obstruct any Cerenkov light from those air showers accepted. The net result of this was to reduce the night sky noise, thus allowing reliable measurements to be made to lower photon densities. The modified system was operated at Woomera (altitude 166 m, tilted at 10° to the zenith) during the March 1985 new moon period. The results from this run are shown by the solid squares in Fig. 1 and are in excellent agreement with earlier runs at high photon densities. At low photon densities, the results are consistent with the corrected Alice Springs data except for the lowest two points (plotted as open squares) which are affected by night sky noise.

4. Data Analysis. For each event, the digitizer outputs from the two density measuring detectors were read by the computer and converted to photon densities using the calibration results. The lower of the photon densities was binned in photon density on a logarithmic scale. During the readout and analysis, the system was automatically inhibited and was de-inhibited by the computer on completion of its analysis. This resulted in a dead-time of ~0.3 s per event. An internal clock recorded the live time. Although each event is accurately calibrated, the discriminator threshold varied during the run due to gain drifts and changing night sky brightness within the field of view. For each run, only events with photon densities well above the discriminator threshold were included in the final analysis. The acceptance solid angle was calculated from the pre-set discriminator output pulse widths and delays. Thus, for each run the exposure (live time x solid angle) and minimum acceptable photon density were determined. The data from separate runs were then combined to obtain the results shown in Fig. 1. Our final result based on those data of Fig. 1 which were unaffected by night sky noise are replotted in Fig. 2.

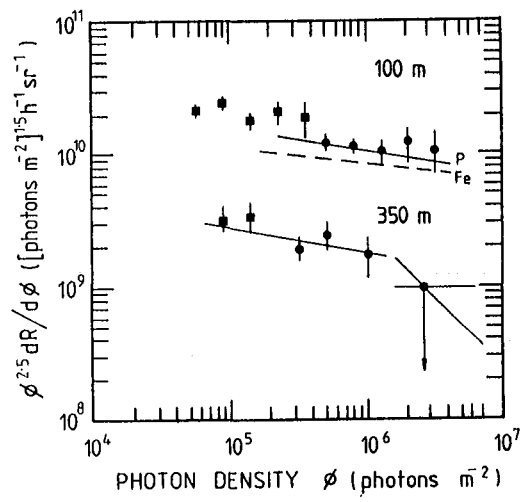

Fig. 2. Photon density spectrum data from Fig. 1 which are not subject to biasses due to night sky noise. Points with large error bars are also omitted for clarity. A power-law fit to the 350 m data is plotted. Upper limits to power law spectra above 1.6×10^6 photons m^{-2} are also plotted. Expected 100 m photon density spectra based on the cosmic ray energy spectrum obtained from the 350 m data are plotted for two extreme assumptions about the nuclear mass composition.

5. Discussion. We can derive the primary cosmic ray energy spectrum from the 350 m data independently of the nuclear mass composition. The 350 m photon density spectrum data of Fig. 2 up to 10^6 photons m^{-2} are well fitted by a power law in photon density. The best fit is indicated in the figure and has a differential index of $\gamma_\phi = 2.7\pm0.2$. Above 1.6×10^6 photons m^{-2}, no events were recorded, indicating a steepening in the cosmic ray spectrum, and 1σ upper limits to power law spectra above this photon density have been plotted in Fig. 2 for γ_ϕ ranging from 2.5 to 3.5. Using Fig. 9(a) of ref. 1, which relates γ_ϕ to γ_E for different spacings, this corresponds to a spectral index $\gamma_E = 2.72 \pm 0.2$ for the cosmic rays. The cosmic ray energy spectrum in the energy range 3×10^{15} - 3×10^{16} eV (corresponding to 10^5-10^6 photons m^{-2} for the 350 m system) may then be obtained directly with the aid of Figs. 8 and 9(b) of ref. 1 which relate photon density to primary energy and the absolute fluxes. The result is shown in Fig. 3 where it is compared with previous measurements of the cosmic ray energy spectrum. Our result is consistent with the extrapolation to lower energies of the Haverah Park data if there is a steepening of the spectrum at ~3×10^{16} eV. Comparison with balloon and satellite data at

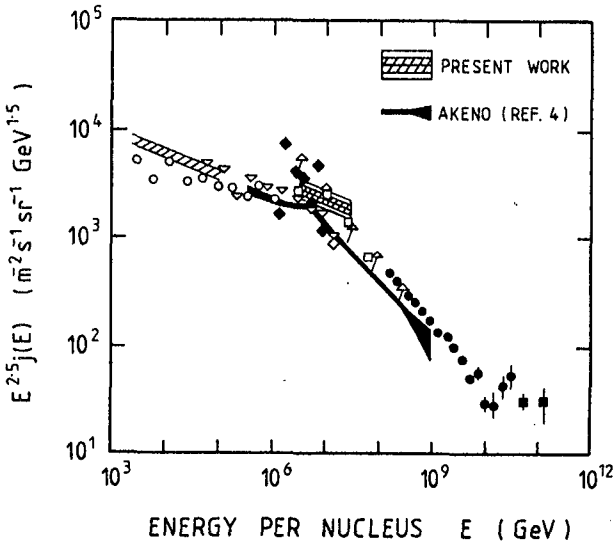

Fig. 3 Primary cosmic ray energy spectrum measurements (see ref. 3 for key to data). Our result at $3x10^{15}$-$3x10^{16}$ eV is indicated and is subject to statistical and systematic errors each of about 10%.

lower energies would indicate the presence of a "kneecap". The Akeno data also indicate the presence of a kneecap but at a factor of ~3 to 5 lower energy.

For the cosmic ray energy spectrum we derived from the 350 m data, we can predict the photon density spectrum for the 100 m system assuming different nuclear mass compositions with no other adjustments being made. This has been done for two extreme assumptions, 100% protons or 100% Fe-nuclei, using simulation results similar to those described in ref. 1 but appropriate to the 100 m system. The expected 100 m spectra are plotted in Fig. 2 for comparison with the data. (Note that for the 100 m system, $3x10^{15}$-$3x10^{16}$ eV corresponds to higher photon densities than for the 350 m system.) Unfortunately, with the detectors moved apart to 100 m some sensitivity to composition is lost (all sensitivity is lost for 350 m). Also, because of the relatively low power law index of the cosmic ray spectrum in this energy range the two curves are rather close together. Nevertheless, the data appear to favour a relatively light composition although a heavy composition is not ruled out. More data would be required to resolve this question. Whatever the composition, however, provided it remains unchanged down to $\sim10^{15}$ eV, the 100 m data would indicate that the cosmic ray spectrum we derived between $3x10^{15}$ and $3x10^{16}$eV continues unchanged down to $\sim10^{15}$ eV.

6. Acknowledgements. We are grateful to Professor J. Thomas of the Physics Department of the R.A.A.F. Academy for use of facilities at Alice Springs, and to the Area Administrator of D.S.C. Woomera for facilities at Woomera. This work has been supported in part by grants from the University of Adelaide and the A.R.G.S. and by provision of a Queen Elizabeth II Fellowship and Research Support Grant to R.J.P.

References.

1. R.J. Protheroe and J.R. Patterson, 1984: J. Phys. G: Nucl. Phy., 10, 841.
2. A.G. Gregory, J.R. Patterson and B.R. Dawson, 1983: Proc. 18th ICRC (Bangalore), 8, 145.
3. R.J. Protheroe, 1984: J. Phys. G: Nucl. Phys., 10, L99.
4. M. Nagano et al., 1984: J. Phys. G: Nucl. Phys., 10, 1295.